Predictive Encoding of Contextual Relationships for Perceptual Inference, Interpolation and Prediction

Mingmin Zhao[1,3], Chengxu Zhuang[2,3], Yizhou Wang[1], Tai Sing Lee[3]
[1] Computer Science Department, Peking University, Beijing, China
[2] Electrical Engineering Department, Tsinghua University, Beijing, China
[3] Center for the Neural Basis of Cognition and Computer Science Department, Carnegie Mellon University, Pittsburgh, U.S.A.
{Mingmin.Zhao, Yizhou.Wang}@pku.edu.cn, zcx11@mails.tsinghua.edu.cn, tai@cnbc.cmu.edu

Abstract

We propose a new neurally-inspired model that can learn to encode global relationship context of visual events across time and space and to use the contextual information to modulate the analysis by synthesis process in a predictive coding framework. The model is based on the principle of mutual predictability. It learns latent contextual representations by maximizing the predictability of visual events based on local and global context information. The model can therefore interpolate missing events or predict future events in image sequences. The contextual representations modulate the prediction synthesis process by adaptively rescaling the contribution of each neuron's basis function. In contrast to standard predictive coding models, the prediction error in this model is used to update the context representation but does not alter the feedforward input for the next layer, thus is more consistent with neuro-physiological observations. We establish the computational feasibility of this model by demonstrating its ability to simultaneously infer context, as well as interpolate and predict input image sequences in a unified framework.

Introduction

In theoretical neuroscience, it has been proposed that in order to process rapidly the constant influx of sensory inputs, which are complex, noisy and full of ambiguity, the brain needs to learn internal models of the world, and use them to generate expectations and predictions based on memory and context to speed up and facilitate inference. Comprehension is achieved when the synthesized prediction or expectation, mediated by recurrent feedback from the higher visual areas to the early visual areas, explains the incoming signals (Mumford 1992). This framework was recently popularized by (Rao and Ballard 1999) in psychology and neuroscience as the predictive coding theory, and can be understood more generally in the framework of hierarchical Bayesian inference (Lee and Mumford 2003; Dean 2005; Friston 2005; George and Hawkins 2006). The predictive coding idea has been generalized to non-visual systems (Bar 2007; Todorovic et al. 2011), and even a "unified theory" of the brain (Friston 2010). The computational utility of these conceptual models remains to be elucidated.

Boltzmann machines, Helmhotlz machine, and more recently deep belief nets (Hinton and Sejnowski 1986; Hinton, Osindero, and Teh 2006) might be the closest real computational models demonstrating this idea, as these models also learn internal models of the world based on the principle of matching the statistical correlation of the observed data and the hidden nodes with that of the hidden nodes and the prediction during unsupervised learning. However, while deep learning models exploit feedback prediction during unsupervised learning, inference in deep network relies mostly on fast feed-forward computation. Moreover, deep learning networks learn feature hierarchy that has been useful for object classification (Hinton, Osindero, and Teh 2006; Vincent et al. 2008; Lee, Ekanadham, and Ng 2008). Yet, they have not been fruitfully used to explain visual perception. Perceptual inference is a constructive and generative process. That is, we do not simply extract features from the visual input for recognition, but actively reconstruct a representation of the world based on the ambiguous input, as well as memory and contextual information. Numerous physiological studies have demonstrated the importance of contextual influence even in the activities of V1 neurons (Lee and Mumford 2003; Schwartz, Hsu, and Dayan 2007; Haslinger et al. 2012). Kelly et al. (2010) and others for example demonstrated that the activities of the local field potential and of the surrounding neurons could predict better V1 neurons' responses than the receptive field stimuli!

In this work, we propose a new framework that can learn internal models of contextual relationships between visual events in space and time. These internal models of context, learned as latent variables, then modulate the prediction synthesis process by rescaling the basis functions represented by the neurons multiplicatively in the framework of predictive coding. Our model is also related to Memisevic and Hinton's (Susskind et al. 2011; Memisevic 2011) gated Boltzmann machines which also model temporal relationship context in image sequences. Their gated machine, modeling 3-way multiplicative interaction, makes strong assumption on the role of neural synchrony utilized in learning and inference. In addition, it is difficult and expensive to generalize such model for N-way interaction. In our new formulation, synchrony is not required , evidence from 2 or more input frames are summed together as in commonly accepted spatiotemporal filtering of the input signals by V1 neurons. Our framework of predictive coding under contextual modulation allows us to achieve the same and in fact more functions than the gated machines. Our model also advance the predictive coding model in that the residue signals between the prediction and the input are used to update the contextual representation only, and do not replace the feedforward input to the next layer as in standard predictive coding model (Rao and Ballard 1998). Thus, our predictive coding model might be more biologically plausible. In our model, the inference of the context relationship and the inference of the visible units happen simultaneously in a bottom-up and top-down manner to achieve image reconstruction, interpolation and prediction in a unified framework. This provides a viable model for conceptualizing and understanding how contextual modulation can influence the constructive and generative aspects of visual perception.

Description of the Model

The proposed model seeks to learn relationships between visual events in a spatial or temporal neighborhood to provide contextual modulation for image reconstruction, interpolation and prediction. It can be conceptualized as an autoencoder with contextual modulation, or a context-dependent predictive coding model. A predictive coding model states that the brain continually generates models of the world based on context and memory to predict sensory input. It synthesizes a predicted or expected image and feeds back to match the input image represented in the lower sensory areas. The mismatch between the prediction and the input produces a residue signal that can be used to update the top-down models that direct the generative processes until all the meaningful inputs are explained (Mumford 1992, Rao and Ballard 1999). Our model is an extension of the "standard" predictive coding model in that the residue signals (the discrepancy between the visible units and the predicted units) update the relationship context. The contextual representation in turn modulates the image synthesis or prediction process by rescaling (multiplying) the basis functions of the neurons adaptively so that the synthesized or predicted images in a temporal neighborhood maximize their ability to predict each other.

The problem can be formulated as minimizing the following energy function,

$$L(\boldsymbol{x}_{1...T}, \boldsymbol{z}; \boldsymbol{\theta}) = \sum_t \|\boldsymbol{x}_t - \hat{\boldsymbol{x}}_t(\boldsymbol{x}_{1...T}, \boldsymbol{z}; \boldsymbol{\theta})\|_2^2 + \lambda \|\boldsymbol{z}\|_1, \tag{1}$$

where $\boldsymbol{x}_t$ is the input signal, $\hat{\boldsymbol{x}}_t$ is the predicted signal, $\boldsymbol{z}$ is the latent relationship context variables, $\boldsymbol{\theta} = \{\boldsymbol{W}_{1...T}, \boldsymbol{W}^z\}$ is a collection of parameters of the model to be learned, including the basis functions or receptive fields of the neurons, and the modulating basis functions of the latent variables. The second term in the function is a L_1 regularization term that makes the context latent variables sparse, with $\lambda > 0$ serving to balance the importance of the prediction error term and the regularization term.

The objective of the model is to learn a set of relationship contexts that can modulate the prediction to maximize the mutual predictability of the synthesized image across space or time. We will now describe how the prediction can be generated in this model. The model's information flow can be depicted as a circuit diagram shown in Figure 1. It consists of an input (visible) layer $\boldsymbol{x}_t$, a hidden layer $\boldsymbol{y}_t$ that performs spatiotemporal filter operation on the input layer, a prediction layer $\hat{\boldsymbol{x}}_t$ that represents the prediction generated by rescaling of local information $\boldsymbol{y}_t$ by the contextual modulation layer $\boldsymbol{m}$, and a $\boldsymbol{z}$ layer represents the context variables in a compact representation. Residue error signals, shown in a dash line, are propagated back to update context $\boldsymbol{z}$.

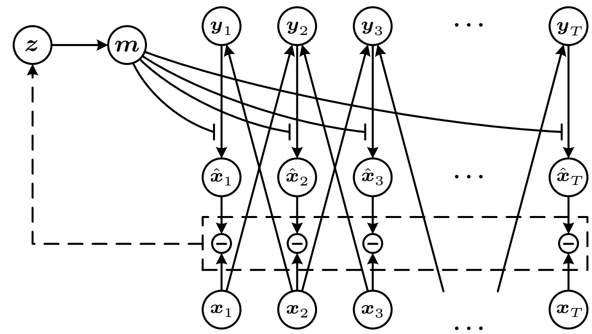

Figure 1: Computational circuit of the *Predictive Encoder*

In the **visible layer**, $\boldsymbol{x}_t \in \mathbb{R}^D, t = 1, ..., T$ denotes a set of visual events. In our experiment, $\boldsymbol{x}_t$ is essentially an image, and $\boldsymbol{x}_{1...T}$ is a sequence of video images. Notice that in the visible layer it is not necessary for all the visual events to be present, since the model possesses the ability to predict or generate the missing events from available partial observations based on the principle of mutual predictability.

In the **hidden layer**, $\boldsymbol{y}_t \in \mathbb{R}^B, t = 1, ..., T$ is defined as

$$\boldsymbol{y}_t = \sum_{\tau \in \mathcal{N}(t)} \frac{1}{|\mathcal{N}(t)|} \boldsymbol{W}_\tau \boldsymbol{x}_\tau, \tag{2}$$

where $\mathcal{N}(t)$ defines the index set of $\boldsymbol{x}_t$'s neighbors and $|\cdot|$ returns the size of a set. $\boldsymbol{W}_t \in \mathbb{R}^{B\times D}, 1 \le t \le T$ is weight matrix to be learned as parameters. Each row of $\boldsymbol{W}_t$ can be viewed as a feature filter for a particular visual event in an image frame t. It can be considered as feedforward input to a neuron based on its spatial receptive field at a particular time frame. For each t, there are B number of hidden units, $(y_t^1, ...y_t^B)$. A particular sequence of related W_t for unit i is the **spatiotemporal filter** receptive field of a neuron i whose feedforward input is characterized by y_t^i as the response of its spatiotemporal filter at frame t to a particular sequence of image frames in a temporal neighborhood. Our definition of the neighborhood is flexible. The temporal neighborhood can be made causal, including up to frame t, or $t-1$ and the model would still work. Here, we use this non-causal symmetrical neighborhood to demonstrate the general computational ability of the model, as it is also relevant for modeling spatial context, and we would like to perform interpolation – modifying our interpretation of the past events based on present evidence and recent history.

Spatiotemporal filtering can achieve smoothing and bringing in local neighborhood information to generate the prediction. This by itself potentially can remove noise or achieve dimensionality reduction as in the case of autoencoder or independent component analysis, but cannot provide global relationship contextual information to modulate the prediction process. To allow the model to learn relationship context, we introduce two sets of latent variables: $\boldsymbol{m} \in \mathbb{R}^B$ the modulator latent variables and the relationship context latent variables $\boldsymbol{z}$. A particular modulator in $\boldsymbol{m}$ is a latent variable associated with the transformation of a visual pattern across frames. It ties together related a set of feature detectors, one from each frame, in the temporal neighborhood into a spatiotemporal filter. Its activity is emitted by the contextual representation $\boldsymbol{z}$ to rescale the contribution of its associated neuron's feedforward response activity y_t^i to generate, in conjunction with other neurons in the hidden layer, the prediction signal $\hat{\boldsymbol{x}}_t$. It can be considered a multiplicative top-down modulation signal acting on a neuron in the hidden layer from the contextual representation $\boldsymbol{z}$. The modulator is content-specific, as it is associated with the transformation of a particular visual event or feature over time. The context variable $\boldsymbol{z}$ is content-invariant. It is a compact representation of $\boldsymbol{m}$, representing for example a particular motion velocity regardless of the features in the movie. $\boldsymbol{m}$ and $\boldsymbol{z}$ are related by

$$\boldsymbol{m} = \boldsymbol{W}^z \boldsymbol{z}, \tag{3}$$

where $\boldsymbol{W}^z$ is a set of basis functions mapping context $\boldsymbol{z}$ to the activity of all the $\boldsymbol{m}$ modulators. The prediction $\hat{\boldsymbol{x}}_t$ in the prediction layer is given by

$$\hat{\boldsymbol{x}}_t = {\boldsymbol{W}_t}^{\mathrm{T}}(\boldsymbol{y}_t \odot \boldsymbol{m}), \tag{4}$$

where $\odot$ is an element-wise product, and thus the contribution of each neuron to the predicted $\hat{\boldsymbol{x}}_t$ is its feedforward input rescaled by context modulation $\boldsymbol{m}$ to generate a weight for its spatial basis function $\boldsymbol{W}_t$. $\hat{\boldsymbol{x}}_t$ is the sum of the contribution of all the neurons in the hidden layer. Modulator $\boldsymbol{m}$ can be viewed as a high-dimensional distributed representation of relationships, the structure of which is modeled by a low-dimensional context representation $\boldsymbol{z}$ which is made sparse by the sparsity term in the loss function.

Combining all the equations together, the prediction generated by the context-dependent predictive coding model is given by

$$\hat{\boldsymbol{x}}_t(\boldsymbol{x}_{1\ldots T}, \boldsymbol{z}; \boldsymbol{\theta}) = {\boldsymbol{W}_t}^{\mathrm{T}}((\sum_{\tau \in \mathcal{N}(t)} \frac{1}{|\mathcal{N}(t)|} \boldsymbol{W}_\tau \boldsymbol{x}_\tau) \odot \boldsymbol{W}^z \boldsymbol{z}) \tag{5}$$

Computationally, the update of the relationship context latent variables $\boldsymbol{z}$ is driven by the residue signals $\boldsymbol{x}_t - \hat{\boldsymbol{x}}_t$ via backpropagation.

Description of the Algorithms

In this section, we describe the learning and inference algorithms developed for our model.

Unsupervised Parameters Learning

The training dataset is composed of n image sequences $\{\boldsymbol{x}^{(1)}_{1\ldots T}, ..., \boldsymbol{x}^{(n)}_{1\ldots T}\}$ and we assume each of them to be an i.i.d sample from an unknown distribution. The objective is to optimize the following problem:

$$\underset{\boldsymbol{\theta}, \boldsymbol{z}}{\text{minimize}} \quad \sum_{i=1}^{n} L(\boldsymbol{x}^{(i)}_{1\ldots T}, \boldsymbol{z}^{(i)}; \boldsymbol{\theta}), \tag{6}$$

We adopt an EM-like algorithm that updates parameters and imputes hidden variable $\boldsymbol{z}$ alternatively while keeping the other one fixed.

Update $\boldsymbol{\theta}$ We use Stochastic Gradient Descent (SGD) to update $\boldsymbol{\theta}$ based on the following update rule:

$$\boldsymbol{\theta}^{(k+1)} = \boldsymbol{\theta}^{(k)} + \Delta\boldsymbol{\theta}^{(k)} \tag{7}$$

$$\Delta\boldsymbol{\theta}^{(k)} = \eta \frac{\partial}{\partial \boldsymbol{\theta}^{(k)}} (\sum_{s \in S(k)} L(\boldsymbol{x}^{(s)}_{1\ldots T}, \boldsymbol{z}^{(s)}; \boldsymbol{\theta}^{(k)})) + \nu \Delta\boldsymbol{\theta}^{(k-1)} \tag{8}$$

where the free parameter $\eta \in \mathbb{R}^+$ is the learning rate, $S(k)$ defines the mini-batch used for training at time k and $\Delta\boldsymbol{\theta}^{(k-1)}$ is the momentum term weighted by a free parameter $\nu \in \mathbb{R}^+$. The momentum term helps to avoid oscillations during the iterative update procedure and to speed up the learning process. All the free parameters in the experiments are chosen under the guidance of Hinton (2010).

The algorithm is implemented using a python library Theano (Bergstra et al. 2010) which provides highly optimized symbolic differentiation for efficient and automatic gradient calculation with respect to the objective function. The idea of Denoising (Vincent et al. 2008) is also used to learn more robust filters.

Estimate $\boldsymbol{z}$ Given fixed $\boldsymbol{\theta}$, we estimate the hidden context representation $\boldsymbol{z}^{(i)}$ for each sequence by solving the following optimization problem independently and in parallel:

$$\underset{\boldsymbol{z}^{(i)}}{\text{minimize}} \sum_t \|\boldsymbol{x}^{(i)}_t - \hat{\boldsymbol{x}}_t(\boldsymbol{x}_{1\ldots T}, \boldsymbol{z}; \boldsymbol{\theta})\|_2^2 + \lambda \|\boldsymbol{z}^{(i)}\|_1 \tag{9}$$

where $\hat{\boldsymbol{x}}^{(i)}_t$ is computed by Eqn.(5). To better exploit the quadratic structure of the above objective function, we solve this convex optimization problem using a more efficient quasi-Newton method *Limited memory BFGS (L-BFGS)* algorithm instead of gradient descent as suggested by Ngiam et al. (2011).

During the training with each batch of data, we first update the parameter $\boldsymbol{\theta}$ using one step stochastic gradient descent, then iterate at most five steps of L-BFGS to estimate the hidden variable $\boldsymbol{z}$.

Inference with Partial Observation

Inference with partial observation refers to prediction or reconstruction of a missing image given neighboring observed ones in the sequence and the learned parameters $\boldsymbol{\theta}$. This problem is posed as an optimization problem that simultaneously estimates the latent variables $\boldsymbol{z}$ for context representation and the missing event/frame $\boldsymbol{x}_u, 1 \leq u \leq T$:

$$\underset{\boldsymbol{x}_u, \boldsymbol{z}}{\text{minimize}} \quad L(\boldsymbol{x}_{1\ldots T}, \boldsymbol{z}; \boldsymbol{\theta}) \tag{10}$$

This optimization problem can be solved efficiently and iteratively by an alternating top-down and bottom-up estimation procedure. The top-down estimation "hallucinates" a missing event based on the neighboring events and the higher-level context representation. The bottom-up procedure uses the prediction residue error to update the high level understanding of the relationship context. Specifically, minimizing Eqn.(10) is realized by alternately estimating $\boldsymbol{x}_u$ and $\boldsymbol{z}$ iteratively.

Estimate $\boldsymbol{z}$ Given learned $\boldsymbol{\theta}$ and current estimation of $\boldsymbol{x}_u$, we use the same method as Eqn.(9) to estimate $\boldsymbol{z}$.

Estimate $\boldsymbol{x}_u$ Given learned $\boldsymbol{\theta}$ and current estimation of $\boldsymbol{z}$, we estimate a missing event/frame by solving the following optimization problem:

$$\underset{\boldsymbol{x}_u}{\text{minimize}} \sum_{t \in \mathcal{N}(u) \cup \{u\}} \|\boldsymbol{x}_t - \hat{\boldsymbol{x}}_t(\boldsymbol{x}_{1\ldots T}, \boldsymbol{z}; \boldsymbol{\theta})\|_2^2 \tag{11}$$

While Eqn.(5) considers only the prediction of $\boldsymbol{x}_u$, this optimization problem factors the role of $\boldsymbol{x}_u$ in predicting/constructing its neighbors. Notice that this objective function is a standard quadratic function, which has a closed form solution in one step. For a video sequence, predicting a future frame and interpolating a missing frame are formulated and can be accomplished in an unified framework.

Experimental Results

Receptive Field Learning

In the first experiment, we trained our model using movies synthesized from natural images. Each movie sequence exhibited either translation, rotation or scaling transformation. We trained models for each type of transformation movies independently, as well as the mixture of the three. We will show results of the feedforward filters $\boldsymbol{W_t}$ from models trained with three frames. The algorithm, however, is not limited to three frames and we will show results of the model trained with relatively longer sequences such as six frames.

The images used to generate the training movie sequences were random samples from the whitened natural images used in Olshausen and Field (1997). For translation, the patch size was 13×13 and the elements of shift vectors were sampled from the interval [-3, 3] (in pixels) uniformly. For rotation, the patch size was 13×13 and the rotation angles were uniformly sampled from $[-21°, 21°]$ at $3°$ intervals. For scaling, the patch size was 21×21 and the scaling ratio was uniformly sampled from $[0.6, 1.8]$. For mixture of motion, the patch size was 21×21. The training set was simply a combination of all three types of single-transformation movies, each with a constant transformation parameter. For models trained by a single type of motion, we used 100 modulator units in $\boldsymbol{m}$ and 25 context representation units in $\boldsymbol{z}$ and 20000 training sequences. For the models trained with all three types of motions, we used 300 modulator units and 75 context representation units and 30000 training sequences. We used unsupervised parameters learning algorithm describe before with a learning rate (η) of 0.05 and momentum (ν) 0.5. Every model was trained for 500 epochs.

Figure 2(a) shows that the filters learned from translation are Fourier basis with quadrature phase difference between frames. Figure 2(b) shows that the filters learned from rotation are Fourier basis in polar coordinates, also with a quadrature phase in polar angle between frames. The filters learned from scaling shown in Figure 2(c) depicts filters trained by scaling. They resemble rays emanating from the center or shrinking circles, reflecting the trajectories of points during scaling. Figure 2(d) shows the filters trained with motion mixture, which appear to encode the transformations in a distributed manner using localized Gabor filters, similar to receptive fields of V1 neurons. Figure 2(e) shows the filters trained with 6 frames rotation sequences. This demonstrates the model can be used to learn long sequence filters.

Decoding Motion from Context Representation

Next, we show that our context latent variables encode transformation or motion information by (1) classifying a test sequence into one of the three types of motion using SVM, (2) decoding the motion parameters using linear regression, (3) computing optical flow in natural movies in the UCF sports action data set (Rodriguez, Ahmed, and Shah 2008). In all three tests, we used the context representation of a model trained simultaneously with mixture of all three types of motion sequences as the features.

Classifying the type of transformation: We trained three SVMs, one for each type of transformation. For each test sequence, we inferred the context representation $\boldsymbol{z}$, and then computed the probability of the three SVMs and chose the classification with the highest probability. All the SVMs were trained using the dot product as kernel function only. The confusion matrix shown in Table 1 suggests that the context representation does encode the content-invariant transformation information.

	Rotation	Translation	Scaling
Rotation	9369	144	392
Translation	427	9773	330
Scaling	204	83	9278

Table 1: Confusion Matrix: first column is predicted labels

Decoding parameters of the transformation: We trained a linear regression model using the context representation $\boldsymbol{z}$ as the regressor to predict/estimate the transformations, namely, velocity for translation, angular velocity for rotation and scaling ratio for scaling. Let ρ denote the three transformation parameters, and the relative regression error of the estimations is defined as $\frac{|\rho_{groundtruth} - \rho_{predicted}|}{|\rho_{groundtruth}|}$. The CDFs of relative regression error of the estimates in Figure 3 shows that the context representation does contain information about the parameters of the transformation as well.

Estimating optical flow in natural movies: To compute the optical flow in a sequence of images, we took patches from the sequences, and fed every pair of the corresponding image patches extracted from the same location of two successive frames to the proposed predictive encoder, then computed the context representation $\boldsymbol{z}$ for the patch pairs. Finally, we applied the regression model learned above to estimate the transformation of the patches and derive the optical flow.

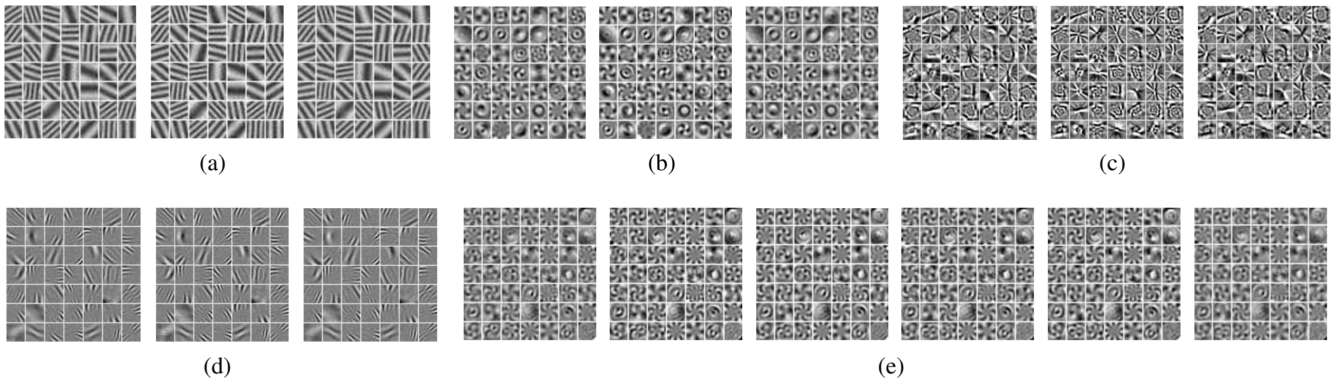

Figure 2: Filters learned from: (a) Translation, (b) Rotation, (c) Scaling, (d) Mixture of Transformations, (e) 6-frame Rotation.

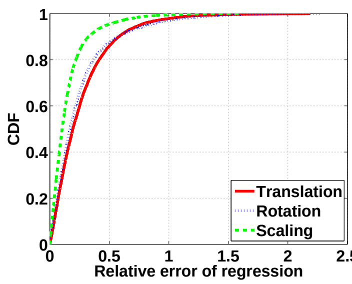

Figure 3: CDFs of relative regression error.

Figure 4: Optical flow from regression.

The results shown in Figure 4 demonstrated that the context representation by itself is sufficient to provide optical flow information. This suggests those context units are encoding content-invariant motion information either individually or in a distributed representation.

Prediction and Interpolation

The most crucial test of the model is its ability to predict and interpolate. We first illustrate its interpolation and prediction using training sequences generated from three datasets: face images (Gourier, Hall, and Crowley 2004), MNIST handwritten digits and natural images (Olshausen and Field 1997) and then we will show results of learning 3D rotation on NORB dataset (LeCun, Huang, and Bottou 2004).

First, we applied one of the three transformations to an image drawn from three datasets to generate another transformed images and formed an image pair. Then we applied our context-dependent predictive edcoder, trained using the mixture transformation sequences of natural images in the previous section, to the image pair. When the image pairs were input to the nodes $\boldsymbol{x}_1$ and $\boldsymbol{x}_2$, the latent variables $\boldsymbol{z}$ was inferred, and a $\boldsymbol{x}_3$ was simultaneously estimated as the prediction by the model.

Figure 5: Prediction results (third row) generated by the model based on the first two rows of frames.

Figure 5 shows the results of predictions given the first and second frames. They demonstrated the predictive coding model's ability to accomplish prediction using a top-down bottom-up algorithm. These findings also show the context representation $\boldsymbol{z}$ has encoded content-invariant transformation relationships that can be used to provide context modulation to generate prediction.

Interpolation can be accomplished in the same way - just feed the input image pair to the nodes $\boldsymbol{x}_1$ and $\boldsymbol{x}_3$ of the model. The second row of Figure 6 shows the interpolation results given the frame pair on the first and the third rows.

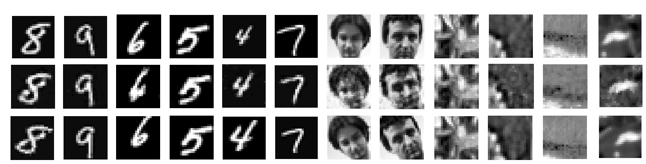

Figure 6: Interpolation results (second row) generated by the model based on the other two rows of frames.

Next, we tested our model with a more challenging NORB dataset that has images of objects in 3D rotation and in different views and lighting conditions. There were 5 categories of objects (animals, human, cars, trucks, planes) with 10 objects in each category taken with camera in 18 directions, 9 camera elevations and under 6 illuminations.

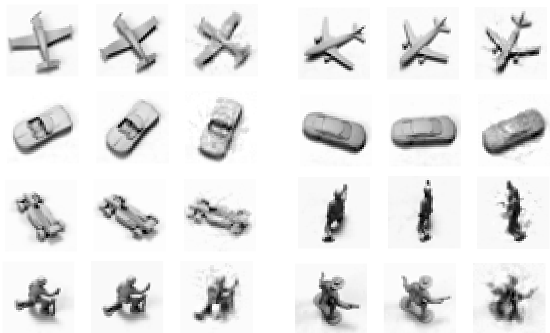

Figure 7: Prediction results (3rd, 6th columns) of NORB

We trained a model for each of the five object categories. Within each category, the data were divided into a training set and a test set based on their elevations. The test set for each model included all the images taken at two particular elevations (4th and 6th), and the training set included image sequences taken at the 7 other elevations. At each elevation, the camera was fixed and the object was rotating in 3D across frames. To train the model for each category, we took sequences of three successive frames (each representing a view from a particular azimuth) of each object in a camera and lighting condition to learn a 3-input model. We tested the model with two input images in a sequence taken from one of the untrained elevations. The prediction results of NORB dataset were obtained in a similar manner for the face and digit cases by presenting the image frames to $\boldsymbol{x}_1$ and $\boldsymbol{x}_2$ to infer $\boldsymbol{z}$ and $\boldsymbol{x}_3$ simultaneously. The results of the prediction are shown in the third column of each object instance in Figure 7. For all prediction and interpolation results, we normalized the output images by making sure the pixel histogram of the output image was matched to the histograms of the input images using histogram matching technique.

Training the model to do interpolation for this database requires an additional measure. The model trained with three consecutive frames will have quadrature phase filters between frames. Thus, the filters for $\boldsymbol{x}_1$ and $\boldsymbol{x}_3$ have a phase shift 180 degrees and thus form a separable spatiotemporal filter, which cannot determine the direction of the motion, resulting in failed interpolation. To overcome this problem and to get a spatiotemporal filter with finer temporal resolution for the hidden layer units, we first trained $\boldsymbol{x}_1$ and $\boldsymbol{x}_3$ to learn quadrature pairs between them, and then trained the filter for $\boldsymbol{x}_2$ with the trained filters for $\boldsymbol{x}_1$ and $\boldsymbol{x}_3$ fixed. The resulting spatiotemporal filters for the three input nodes can then produce reasonable interpolation results, as shown in Figure 8 . A more elegant solution to this problem requires further investigation.

Discussion

In this paper, we have presented a new predictive coding framework that can learn to encode contextual relationships to modulate the prediction synthesis process. In Mumford's (1992) theory or Rao and Ballard's (Rao and Ballard 1999) Kalman-filter version of the predictive coding model, prediction errors are fed forward to the next hidden layer to update the top-down hypotheses. In our model, the feedforward filter input $\boldsymbol{y}_t$ to the next layer is not changed; only the context variables $\boldsymbol{z}$ are updated by the prediction error This distinction is important conceptually because there is little evidence that the feedforward input becomes the residue signals over time. On the contrary, most neurophysiological observations suggested that feedforward signals are usually sustained, though often times habituated some what over time. Our model, by hypothesizing the existence of a small number of interneurons that can encode contextual relationships compactly to modulate prediction generation process, potentially can resolve this dilemma in the current predictive coding models.

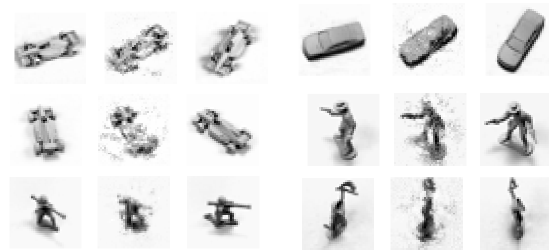

Figure 8: Interpolation results (2nd, 5th columns) of NORB

Our model share some similarities with the autoencoder model but differs in that (1) our model uses context representation to gate the prediction synthesis process while autoencoder does not utilize context, (2) autoencoder relies solely on fast feed-forward computation while our model utilizes a fast top-down and bottom-up procedure to update context and contextual modulation to achieve inference. Our model also shares similar goals with the gated Boltzmann machine in learning transform relationships but our model utilizes a different mechanism. The feedforward connections to the hidden layers in our model are simply performing spatiotemporal filtering, integrating information from N frames without the need for N-way multiplicative interaction as required in the gated machines or require synchrony in neural implementation. Our model therefore can handle 2 or more input frames easily, and can thus utilize top-down bottom-up strategy to infer both the context latent variables as well as the input, which allow us to perform inference, interpolation and prediction in an unified framework.

Our positive experimental results demonstrate the computational feasibility of our framework. The contextual variables $\boldsymbol{z}$ can be stacked up in a hierarchy, as in Memisevic's (2014) transformation of transformation, though it is not clear whether it can go beyond two layers in that scheme. More likely, contextual relationships can be learned between higher order features in the feature hierarchy constructed on $\boldsymbol{y}$, as in deep belief nets, to model higher order spatial and temporal relationship context. Contextual modeling in this framework might allow the modeling of composition of flexible parts, providing a bridge between current deep learning networks with hierarchical compositional models (Zhu and Mumford 2006). Thus, it is worthwhile to explore the proposed model as a new module for deep learning networks.

References

[Bar 2007] Bar, M. 2007. The proactive brain: using analogies and associations to generate predictions. *Trends in cognitive sciences* 11(7):280–289.

[Bergstra et al. 2010] Bergstra, J.; Breuleux, O.; Bastien, F.; Lamblin, P.; Pascanu, R.; Desjardins, G.; Turian, J.; Warde-Farley, D.; and Bengio, Y. 2010. Theano: a cpu and gpu math expression compiler. In *Proceedings of the Python for scientific computing conference (SciPy)*, volume 4, 3.

[Dean 2005] Dean, T. 2005. A computational model of the cerebral cortex. In *Proceedings of the National Conference on Artificial Intelligence*, volume 20, 938. Menlo Park, CA; Cambridge, MA; London; AAAI Press; MIT Press; 1999.

[Friston 2005] Friston, K. 2005. A theory of cortical responses. *Philosophical transactions of the Royal Society B: Biological sciences* 360(1456):815–836.

[Friston 2010] Friston, K. 2010. The free-energy principle: a unified brain theory? *Nature Reviews Neuroscience* 11(2):127–138.

[George and Hawkins 2006] George, D., and Hawkins, J. 2006. Belief propagation and wiring length optimization as organizing principles for cortical microcircuits. Technical report, Numenta.

[Gourier, Hall, and Crowley 2004] Gourier, N.; Hall, D.; and Crowley, J. L. 2004. Estimating face orientation from robust detection of salient facial structures. In *FG Net Workshop on Visual Observation of Deictic Gestures*, 1–9. FGnet (IST–2000–26434) Cambridge, UK.

[Haslinger et al. 2012] Haslinger, R.; Pipa, G.; Lima, B.; Singer, W.; Brown, E. N.; and Neuenschwander, S. 2012. Context matters: the illusive simplicity of macaque v1 receptive fields. *PloS one* 7(7):e39699.

[Hinton and Sejnowski 1986] Hinton, G. E., and Sejnowski, T. J. 1986. Learning and relearning in boltzmann machines. *Cambridge, MA: MIT Press* 1(282-317):4–2.

[Hinton, Osindero, and Teh 2006] Hinton, G.; Osindero, S.; and Teh, Y.-W. 2006. A fast learning algorithm for deep belief nets. *Neural computation* 18(7):1527–1554.

[Hinton 2010] Hinton, G. 2010. A practical guide to training restricted boltzmann machines. *Momentum* 9(1):926.

[Kelly et al. 2010] Kelly, R.; Smith, M.; Kass, R.; and Lee, T. S. 2010. Accounting for network effects in neuronal responses using l1 regularized point process models. In *Advances in neural information processing systems*, 1099–1107.

[LeCun, Huang, and Bottou 2004] LeCun, Y.; Huang, F. J.; and Bottou, L. 2004. Learning methods for generic object recognition with invariance to pose and lighting. In *Computer Vision and Pattern Recognition, CVPR 2004. Proceedings of the IEEE Computer Society Conference on*, volume 2, II–97. IEEE.

[Lee and Mumford 2003] Lee, T. S., and Mumford, D. 2003. Hierarchical bayesian inference in the visual cortex. *JOSA A* 20(7):1434–1448.

[Lee, Ekanadham, and Ng 2008] Lee, H.; Ekanadham, C.; and Ng, A. Y. 2008. Sparse deep belief net model for visual area v2. In *Advances in neural information processing systems*, 873–880.

[Memisevic 2011] Memisevic, R. 2011. Gradient-based learning of higher-order image features. In *ICCV 2011*, 1591–1598. IEEE.

[Michalski, Memisevic, and Konda 2014] Michalski, V.; Memisevic, R.; and Konda, K. R. 2014. Modeling sequential data using higher-order relational features and predictive training. *CoRR* abs/1402.2333.

[Mumford 1992] Mumford, D. 1992. On the computational architecture of the neocortex. *Biological cybernetics* 66(3):241–251.

[Ngiam et al. 2011] Ngiam, J.; Coates, A.; Lahiri, A.; Prochnow, B.; Le, Q. V.; and Ng, A. Y. 2011. On optimization methods for deep learning. In *Proceedings of the 28th ICML-11*, 265–272.

[Olshausen and Field 1997] Olshausen, B. A., and Field, D. J. 1997. Sparse coding with an overcomplete basis set: A strategy employed by v1? *Vision research* 37(23):3311–3325.

[Rao and Ballard 1999] Rao, R. P., and Ballard, D. H. 1999. Predictive coding in the visual cortex: a functional interpretation of some extra-classical receptive-field effects. *Nature neuroscience* 2(1):79–87.

[Rodriguez, Ahmed, and Shah 2008] Rodriguez, M.; Ahmed, J.; and Shah, M. 2008. Action mach a spatio-temporal maximum average correlation height filter for action recognition. In *Computer Vision and Pattern Recognition, 2008. CVPR 2008. IEEE Conference on*, 1–8.

[Schwartz, Hsu, and Dayan 2007] Schwartz, O.; Hsu, A.; and Dayan, P. 2007. Space and time in visual context. *Nature Reviews Neuroscience* 8(7):522–535.

[Susskind et al. 2011] Susskind, J.; Memisevic, R.; Hinton, G.; and Pollefeys, M. 2011. Modeling the joint density of two images under a variety of transformations. In *CVPR 2011*, 2793–2800. IEEE.

[Todorovic et al. 2011] Todorovic, A.; van Ede, F.; Maris, E.; and de Lange, F. P. 2011. Prior expectation mediates neural adaptation to repeated sounds in the auditory cortex: an meg study. *The Journal of neuroscience* 31(25):9118–9123.

[Vincent et al. 2008] Vincent, P.; Larochelle, H.; Bengio, Y.; and Manzagol, P.-A. 2008. Extracting and composing robust features with denoising autoencoders. In *Proceedings of the 25th international conference on Machine learning (ICML-08)*, 1096–1103.

[Zhu and Mumford 2006] Zhu, S.-C., and Mumford, D. 2006. A stochastic grammar of images. *Foundations and Trends® in Computer Graphics and Vision* 2(4):259–362.